Mineralogical Magazine (2026), **90**, 828–837
doi:10.1180/mgm.2025.10161

CAMBRIDGE UNIVERSITY PRESS

Article

High-pressure phase transition in groutite, MnO(OH)

Roman Gajda[1], Agnieszka Huć[1,2], Piotr Rejnhardt[1], Jan Parafiniuk[2], Pierre Fertey[3] and Krzysztof Woźniak[1]

[1]Faculty of Chemistry, University of Warsaw, Warszawa, Poland; [2]Institute of Geochemistry, Mineralogy and Petrology, Department of Geology, University of Warsaw, Warszawa, Poland; and [3]Synchrotron SOLEIL, L'Orme des Merisiers - Saint Aubin, Gif-sur-Yvette Cedex, France

Abstract

Groutite, α-$Mn^{3+}O(OH)$, is a mineral that belongs to the diaspore group. We used X-ray synchrotron radiation in the pressure range from 0.65(6) GPa to 39.85(8) GPa to collect diffraction data for three single crystals of groutite placed in a diamond anvil cell. Groutite is orthorhombic, space group *Pbnm*. Analysis of the reciprocal lattice planes and the intensities of the measured reflections revealed that above 30 GPa, a phase transformation begins in the structure. This transition is gradual, with observable changes in the intensity of specific reflections, particularly those that are forbidden in the *Cmcm* space group. Although we see significant decreases in the intensities of these reflections, many of them still have intensities significantly greater than zero after the beginning of transformation. This is accompanied by a smooth, continuous shrinkage in the unit cell volume, symmetrization of hydrogen positions, and distortion of the MnO_6 octahedra. Analysis of the reflection intensities confirms that the observed changes are due to structural transformations and not experimental or sample effects. This means that the starting *Pbnm* symmetry is preserved although the mineral transforms as a function of pressure close to the *Cmcm* space-group symmetry. We propose a mechanism for this phase transition in the *Pbnm* space group.

Keywords: groutite; MnOOH; phase transition; high pressure; synchrotron

(Received 29 January 2025 UTC; revised 17 September 2025 UTC; accepted 17 September 2025 UTC; Accepted Manuscript published online: 22 September 2025 UTC)

Introduction

Groutite, is a member of the diaspore group, which has the general formula $M^{3+}O(OH)$. Besides diaspore, AlO(OH), (Hill, 1979; Gajda *et al.*, 2024) this group includes bracewellite, CrO(OH), goethite, α-$Fe^{3+}O(OH)$ (Gualtieri and Venturelli, 1999), montroseite, (V^{3+}, Fe^{2+}, V^{4+})O(OH) (Evans and Block, 1953; Evans and Mrose, 1955), and tsumgallite, GaO(OH) (Schlüter *et al.*, 2003). Groutite was discovered by John Walter Gruner (Gruner, 1947) and named in honour of Frank Fitch Grout (1880–1958), an American petrographer, geologist and mineralogist. The Commission on New Minerals, Nomenclature and Classification of the International Mineralogical Association (IMA-CNMNC) official symbol is Gro (Warr, 2021). Like other members of the diaspore group, groutite crystallizes in the *Pnma* space group of the orthorhombic crystal system (Z = 4). An alternative, though non-standard, space-group setting is *Pbnm*.

There are currently four groutite structures deposited in the Inorganic Crystal Structure Database (ICSD) (Hellenbrandt, 2004). The two earliest entries in ICSD provide only basic information about the groutite structure (Collin and Lipscomb, 1949; Glasser and Ingram, 1968). In these papers, the *Pbnm* setting was used, and we will also use this notation for reasons that will be explained later. The two most recent entries in the ICSD use the *Pnma* setting. The work by Kohler *et al.* (1997) focuses mainly on structural changes triggered by temperature within the range from room temperature (RT) to 325°C. The work by Scheinost *et al.* (2001) describes results from X-ray absorption fine structure (XAFS) and X-ray absorption near-edge spectra (XANES) investigations. However, none of these studies investigated the behaviour of groutite under high pressure. A more complex investigation of groutite structure under high temperature (up to 450°C) and relatively high pressure (up to 5.5 GPa), aimed at determining the equation of state, was conducted by Wiethoff *et al.* (2017). Much higher pressures were achieved during investigations of other members of the diaspore group, such as AlO(OH) and CrO(OH). Friedrich *et al.* (2007a, 2007b) studied the structural compression mechanism and compressibility of diaspore, initially up to 7 GPa (experimental pressure), and later up to 51.5 GPa. Despite the significant pressure of ~50 GPa, the single-crystal X-ray synchrotron data did not reveal any phase transitions within the investigated pressure range. However, as described by Komatsu *et al.* (2006), a phase transition of diaspore from the α to δ phase is possible at quite severe conditions, 18 GPa and 1273 K for 10 hrs. There is also information suggesting that

Corresponding author: Krzysztof Woźniak; Email: kwozniak@chem.uw.edu.pl
Associate Editor: G. Diego Gatta

Cite this article: Gajda R., Huć A., Rejnhardt P., Parafiniuk J., Fertey P. and Woźniak K. (2026) High-pressure phase transition in groutite, MnO(OH). *Mineralogical Magazine* **90**, 828–837. https://doi.org/10.1180/mgm.2025.10161

© The Author(s), 2025. Published by Cambridge University Press on behalf of The Mineralogical Society of the United Kingdom and Ireland. This is an Open Access article, distributed under the terms of the Creative Commons Attribution licence (http://creativecommons.org/licenses/by/4.0), which permits unrestricted re-use, distribution and reproduction, provided the original article is properly cited.

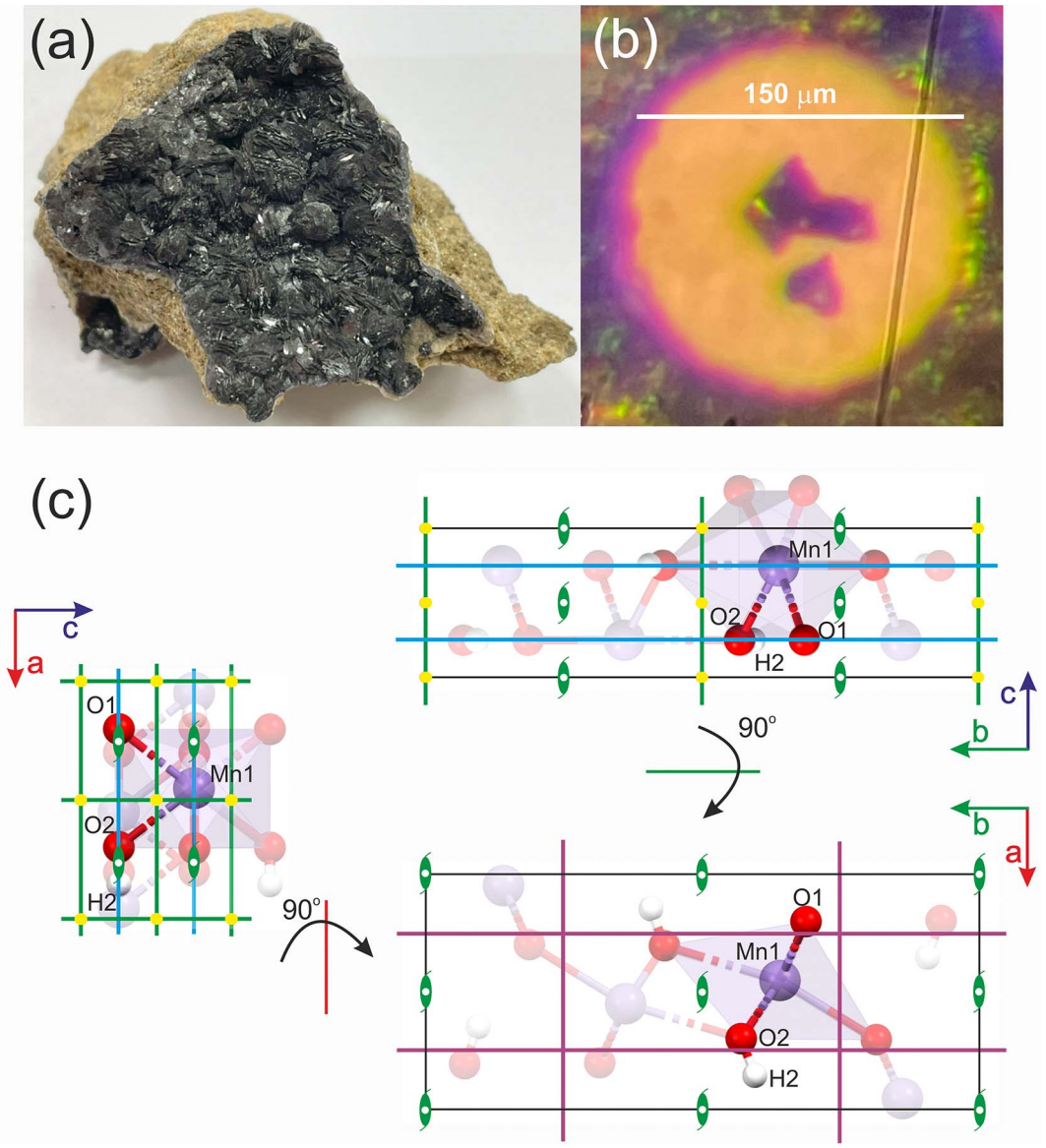


Figure 1. (a) Macroscopic sample of groutite from Zavalye graphite mine, Kirovohrad Oblast, Ukraine (specimen from the private collection of Prof. Jan Parafiniuk, author's photograph). (b) Selected single crystals of groutite (from the same specimen) placed in the DAC. (c) Unit cell with atomic positions (atoms from the asymmetric unit in full colour, others translucent) and symmetry elements: blue lines – mirror planes, purple lines– glides, green lines – twofold screw axis.

another member of the diaspore group, goethite, FeO(OH), may undergo a phase transition at pressure values lower than 50 GPa (Liu *et al.*, 2019). Liu *et al.* presented evidence for pressure-induced phase transitions in goethite at ~7.0 GPa and at ~20.0 GPa.

In addition to groutite (α-Mn^{3+}O(OH)), other manganese hydroxides are also known. Manganite (γ-Mn^{3+}O(OH)) crystallizes in a monoclinic space group $P2_1/c$ (Kohler *et al.*, 1997). It has been investigated within the pressure range up to 12.7 GPa, but no phase transition has been observed (Zhao *et al.*, 2017). Feitknechtite (β-Mn^{3+}O(OH)) is a hexagonal polymorph, but its space group has not yet been determined (Post *et al.*, 2023).

In our work, we have focused on groutite and its potential phase transition triggered by high pressure. Our goal was to investigate changes in the structure within the pressure range from 1 GPa to 50 GPa.

Experimental

The X-ray experiment was conducted using synchrotron radiation at the CRISTAL beamline (wavelength, λ = 0.41691 Å) at the synchrotron facility SOLEIL (Saint-Aubin, France). The investigated mineral sample of groutite was obtained from the Zavalye graphite mine in Kirovohrad Oblast, Ukraine, (see Fig. 1), (Kvasnytsya and Naumenko, 2017). Three selected single crystals of groutite, each in a slightly different orientation, were placed inside a membrane diamond anvil cell (DAC) from BETSA (see Fig. 1). The diameter of the diamond culets was 300 μm. A stainless steel gasket was used, with a hole drilled in the gasket measuring 150 μm before pressure was applied. Helium was used as the pressure medium. Because the gasket hole filled in with helium shrinks significantly during the experiment, the single crystals were placed close to the centre of the culet. Their dimensions are as follows: 36 μm × 25 μm × 20 μm (crystal #1); 40 μm × 21 μm × 20 μm

https://doi.org/10.1180/mgm.2025.10161 Published online by Cambridge University Press

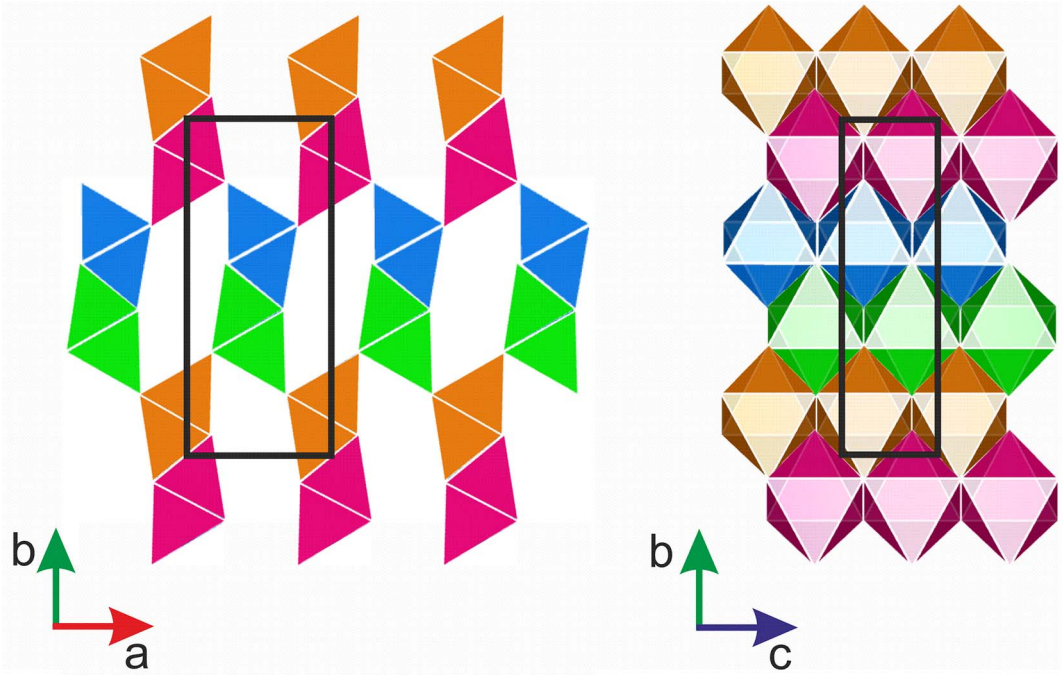


Figure 2. Arrangement of MnO_6 tetrahedra within groutite unit cell at 0.65 (6) GPa, views along: [001] and [100] (from left to right). Black rectangles show the borders of the unit cell.

Table 1. Unit cell parameters of groutite at different pressures

	P (GPa)	*a* (Å)	*b* (Å)	*c* (Å)	*V* (Å^3)
p_1	0.65(6)	4.551(2)	10.6474(6)	2.87392(11)	139.26(7)
p_2	5.86(6)	4.454(4)	10.4449(5)	2.8492(3)	132.54(12)
p_3	10.18(6)	4.389(4)	10.3305(5)	2.8345(3)	128.52(11)
p_4	15.41(6)	4.320(5)	10.2294(6)	2.8186(4)	124.55(14)
p_5	20.62(7)	4.274(7)	10.1349(10)	2.8002(5)	121.3(2)
p_6	25.26(8)	4.238(8)	10.0559(13)	2.7829(6)	118.6(2)
p_7	30.54(8)	4.199(16)	9.9644(18)	2.7690(9)	115.9(4)
p_8	36.15(8)	4.1528(4)	9.8907(14)	2.7306(15)	112.16(7)
p_9	39.85(8)	4.117(9)	9.8540(17)	2.7526(4)	111.7(2)

(crystal #2) and 28 μm × 27 μm × 20 μm (crystal #3). The effective opening angle (2θ) of the setup was ~74°. A ruby chip was used to determine the actual pressure within the chamber. Pressure scale according to Jacobsen *et al.* (2008) was used.

The goal was to achieve pressure values up to ~50 GPa, but the maximum pressure actually achieved was almost 40 GPa. Data were collected at nine pressure points: 0.65(6) GPa, 5.86(6) GPa, 10.18(6) GPa, 15.41(6) GPa, 20.62(7) GPa, 25.26(8) GPa, 30.54(8) GPa, 36.15(8) GPa, and 39.85(8) GPa. At each pressure point, each of the three single crystals was measured separately. Each measurement consisted of three runs, each with a different setup of parameters such as exposure time (1 s or 5.4 s, achieved with attenuators), detector position (θ angle 0° or 15°), and sample rotation using the chi circle (κ angle 0° or 60°). As a result, the dataset collected at each pressure point generally consisted of nine runs (three runs for each of the three measured crystals). Data reduction and merging were carried out using *CrysAlisPro* software (CrysAlis Pro, 2014). The structure was then solved and refined in the *Olex2* program package (Dolomanov *et al.*, 2009), using *ShelXS* and *ShelXL* (Sheldrick, 2008, 2015). Additionally *Jana 2020* software was used to solve and refine disordered structure at 39.85(8) GPa (Petricek *et al.*, 2023). The calculations of reflection intensities, their averaging, grouping and integration were carried out using a script written by RG in the Python programming language.

Results

The crystal structure of groutite is relatively simple and comparable with the structure of diaspore, AlO(OH), (Gajda *et al.*, 2024). The crystal system is orthorhombic (crystal space group *Pbnm*/*Pnma*), with four formula units within the unit cell. The unit cell dimensions are as follows: a = 4.560(2) Å, b = 10.700(5) Å and c = 2.870(1) Å in the *Pbnm* setting (Glasser and Ingram, 1968). Its main building blocks are MnO_6 octahedra. Three mirror and glide planes (***n***, ***m*** and ***a***) pass through each unit cell perpendicularly to X, Y and Z, respectively. All of the atoms are placed on the mirror planes (Fig. 1c). As a result, each atom is at a special position with the occupation factor equal to ½ (this is the site multiplicity). There are one manganese, one hydrogen atom and two types of oxygen atoms (one of them is bonded with hydrogen and the other is not) in the asymmetric part of the unit cell. Each Mn atom is surrounded by six oxygen atoms (three bonded to hydrogen atoms and three not bonded).

In the MnO(OH) structure, the edge-sharing MnO_6 octahedra are organized in rows along the X-direction. Within such a row, the octahedra have the same orientation. Each row of octahedra is connected with three other rows, with one of them sharing edges, and two other sharing vertices. Tunnels in the crystal structure along the Z-axis are formed between the rows connected in this manner.

To simplify this description, we can distinguish four repeating types of rows within the groutite structure (depicted with different colours in Fig. 2). The empty spaces between octahedral ribbons in the crystal structure of groutite, clearly visible along the [001]

https://doi.org/10.1180/mgm.2025.10161 Published online by Cambridge University Press

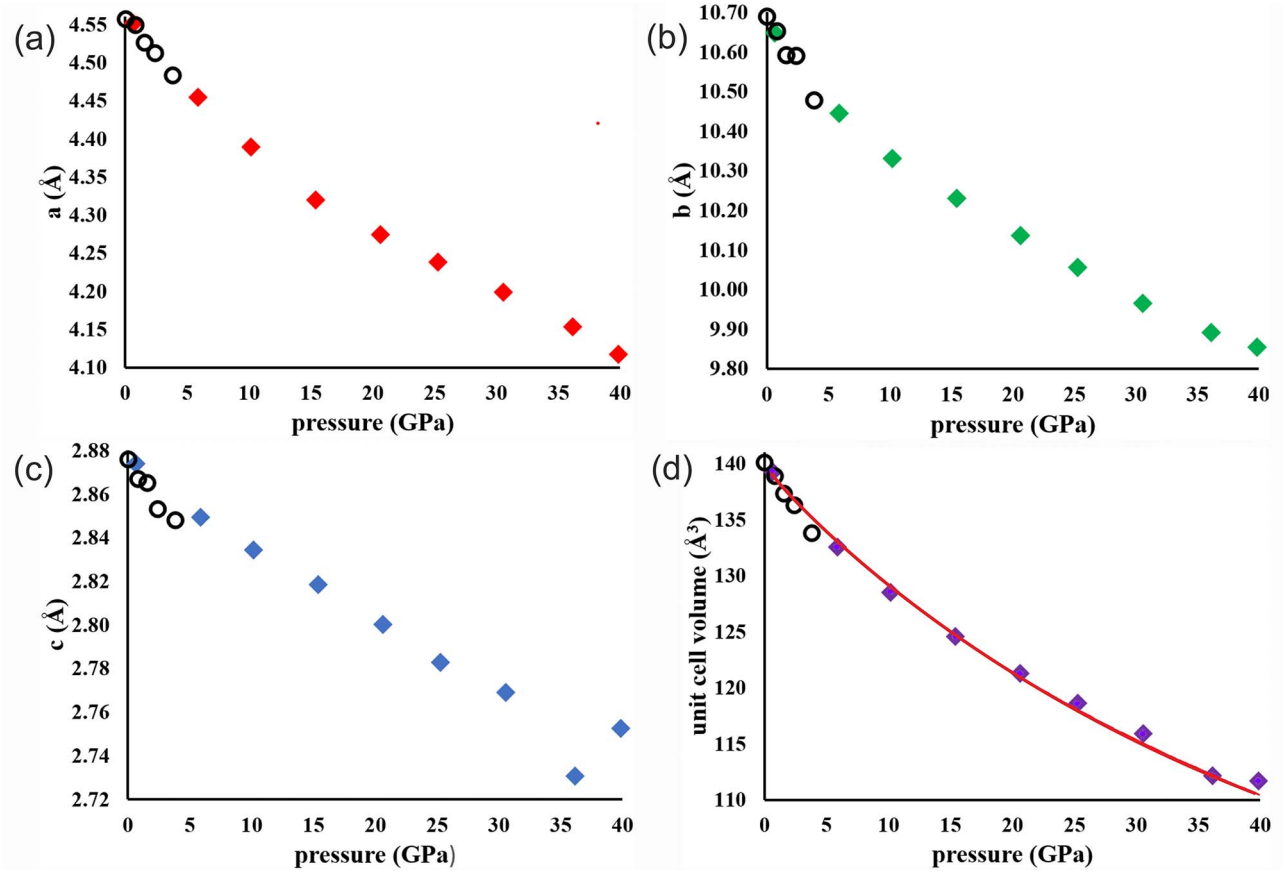


Figure 3. Unit cell dimensions and unit cell volume as a function of pressure. Open circles are literature data points provided by Wiethoff *et al.* (2017). The red solid line in (d) represents the equation of state fitted to the all pressure points.

direction, host H-bonds. However, the H-bonds have been omitted for clarity in Fig. 2.

The unit cell dimensions shrink noticeably (see Table 1) as a function of pressure. Within the pressure range from 0.65(6) GPa to 39.85(8) GPa, the parameter *a* shrinks by about 9.5%, *b* by ~7.5%, *c* by ~4.2%, and the total unit cell volume *V* by ~19.5%. Observed changes of the unit cell parameters correlate very well with those observed by Wiethoff *et al.* (2017) (see Fig. 3). Literature data to prepare Fig. 3 was taken from Table S1 presented in supplementary material corresponding with a publication written by Wiethoff *et al.* (run R06 in this table). Some discrepancies could be perceived for the *c* parameter but we must be aware of the fact that each subfigure has a different scale on the y-axis.

On the basis of collected experimental data presented in Fig. 3, one can fit a third order Birch–Murnaghan equation of state:

$$P = 1.5 * K_T * \left[V_{T,r}^{-7} - V_{T,r}^{-5}\right] * \left[1 - 0.75 * (4 - K_T') * \left(V_{T,r}^{-2} - 1\right)\right]$$

$$\text{Where: } V_{T,r} \equiv \left(\frac{V}{V_{T,0}}\right)^{1/3} \text{ and } V_{T,0} = V_0 exp\left(\int \alpha_{T,0} dT\right)$$

Where: V is the unit cell volume at high pressure P (in GPa) and temperature T (in K), and V_0 is the volume at ambient pressure. $K_T = K + (dK_T/dT)_p \times (T - T_0)$, K'_T and $V_{T,0}$ are the isothermal bulk modulus, its pressure derivative and the unit cell volume at temperature and 0.1 MPa, respectively, $T_0 = 298.15$ K. The thermal expansion at ambient pressure $\alpha_{T,0}$ can be approximated as $\alpha_{T,0} = \alpha + bT$.

Using this method, we obtained the values of the isothermal bulk modulus *K*, its pressure derivative K' and volume at ambient pressure V_0. The fitting procedure was conducted with the use of the *EoSFit7* software (Gonzalez–Platas *et al.*, 2016). The results are as follows: V_0 = 140.0(3) (Å^3), K = 100(6) (GPa) and K' = 4.5(5) (for all nine pressure points, see Fig. 3d) and V_0 = 140.3(1) (Å^3), K = 87(3) (GPa) and K' = 6.8(5) where two pressure points (36.15(8) GPa and 39.85(8) GPa) are excluded. For comparison, the results obtained by Wiethoff *et al.* (2017) for much narrower pressure range from 0 to 5.38 GPa are as follows: V_0 = 139.92 (Å^3), K = 84.0 (GPa) and K' = 4.

One of the noticeable consequence of rising pressure, next to the shrinking of the unit cell dimensions, is the deformation of the MnO_6 octahedra. We tried to describe this deformation by a set

Table 2. Octahedral distortion parameters

	d_{mean} [Å]	ζ [Å]	Δ	Σ [°]	θ [°]
p1	2.039	0.839	0.0060	70.18	180.02
p2	2.014	0.729	0.0046	63.16	158.47
p3	1.999	0.670	0.0039	59.22	147.28
p4	1.984	0.617	0.0034	55.17	136.28
p5	1.971	0.574	0.0030	51.18	126.65
p6	1.960	0.550	0.0028	46.91	117.19
p7	1.948	0.515	0.0025	44.79	111.03
p8	1.932	0.512	0.0026	42.54	103.67
p9	*Split positions of oxygen atoms				

*At this pressure point, we observe disorder among the oxygen atoms; therefore, the distortion parameters have not been determined.

https://doi.org/10.1180/mgm.2025.10161 Published online by Cambridge University Press

Table 3. Details pertaining to the intensity data collections and structure refinements of groutite in *Pbnm* phase at different pressures (λ = 0.41691 Å)

	p1	p2	p3	p4	p5	p6	p7
P (GPa)	0.65(6)	5.86(6)	10.18(6)	15.41(6)	20.62(7)	25.26(8)	30.54(8)
Merged runs	15	8	9	6	6	9	9
Measured reflections	6292	3160	3597	2198	2135	3093	2865
Unique reflections	584	538	523	503	494	483	430
Observed refl. $I > 2\Sigma(I)$	548	487	489	466	457	443	372
R_{int}	0.086	0.044	0.038	0.033	0.035	0.039	0.046
Max. θ (°)	26.2	26.1	26.1	25.9	26.2	26.1	24.6
$(\sin\theta/\lambda)_{max}$ (Å^{-1})	1.061	1.056	1.055	1.049	1.058	1.054	1.000
No. of l.s. parameters	22	22	22	22	22	22	22
$R1$, $I > 2\Sigma(I)$	0.036	0.032	0.028	0.028	0.032	0.037	0.042
$wR2$	0.092	0.082	0.067	0.064	0.105	0.098	0.094
GooF	1.19	1.10	1.12	1.10	1.22	1.19	1.10
Residuals (e^-/Å^3)	1.71, −1.39	0.98, −1.24	1.20, −0.83	1.13, −0.75	1.69, −1.22	1.94, −1.24	1.63, −1.29

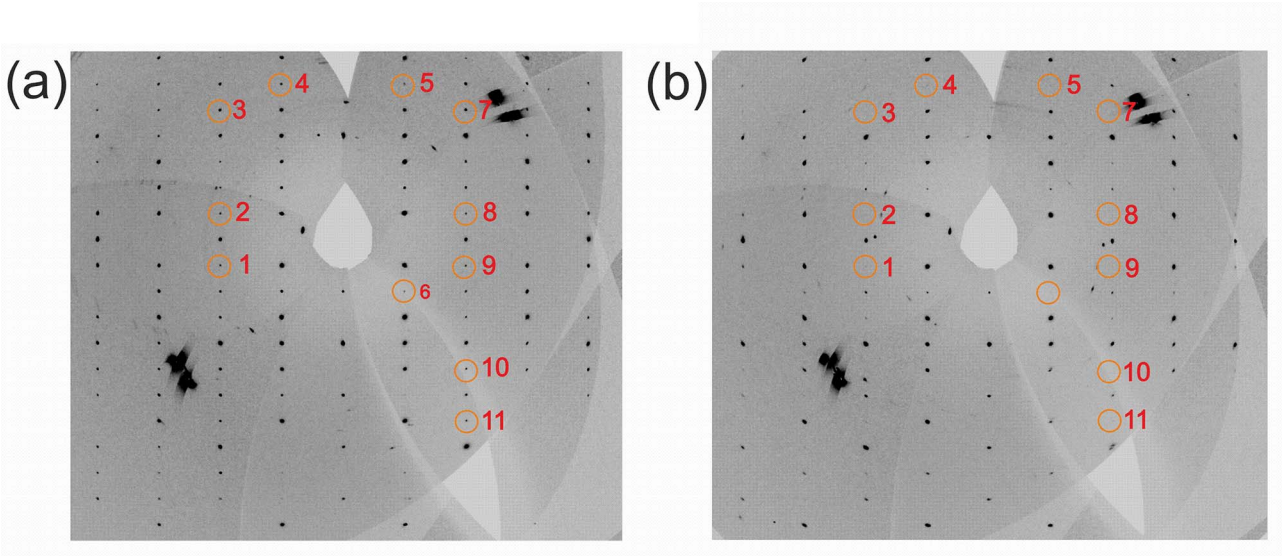


Figure 4. Reconstruction of the 0*Y*Z *0kl* reciprocal lattice plane at (a) 20 GPa and (b) 39 GPa in setting *Pbnm* which corresponds to X*Y*0 *hk0* in setting *Pnma*. Specific systematic extinctions, which fulfils the rule $h + k = 2n+1$ (*Pnma* setting) which corresponds with $k + l = 2n + 1$ (*Pbnm* setting) can be observed. List of encircled reflections: 1) 0,–2,–1; 2) 0,–2,1; 3) 0,–2,5; 4) 0,–1,6; 5) 0,1,6; 6) 0,1,–2; 7) 0,2,5; 8) 0,2,1; 9) 0,2,–1; 10) 0,2,–5; 11) 0,2,–7.

of parameters. Parameter $d_{mean,}$ used in Table 2, refers to the average Mn–O distance in the MnO_6 octahedron. Other parameters such as ζ and Σ are describing stretching, angular and torsional distortions, respectively. Parameters ζ, Δ, Σ and θ are defined as follows:

$$\zeta = \sum_{i=1}^{6} |d_i - d_{mean}|$$

$$\Delta = \frac{1}{6}\sum_{i=1}^{6}\left(\frac{d_i - d_{mean}}{d_{mean}}\right)^2$$

$$\Sigma = \sum_{i=1}^{12} |90 - \varphi_i|$$

$$\theta = \sum_{i=1}^{6} |\theta_i - 60|$$

Parameter ζ is the average of the sum of the deviation of six unique Mn–O bond lengths around the central Mn atom (d_i) from the average value (d_{mean}). Parameter Δ is known as an octahedral distortion parameter (Lufaso and Woodward, 2004). Parameter Σ is the sum of the deviations of 12 unique cis O–Mn–O angles (ϕ_i) from 90°. θ represents a distortion from a perfect octahedral (O_h) to a trigonal prismatic geometry (D_{3h}). All the mentioned parameters were calculated with use of *OctaDist* software (Ketkaew *et al.*, 2021). Information about all Mn–O distances in the MnO_6 octahedra are summarized in Table S1 in Supplementary materials.

Some basic information about the refinement results for the groutite structure in *Pbnm* within the pressure range from 1 to 30 GPa is presented in Table 3. A paragraph explaining the different number of merged runs in different pressure points is in the Supplementary materials. We have applied a riding model in the process of refinement of hydrogen atoms. U_{iso} of H atoms are constrained to 1.2 of the values for the bonded O atoms. Within the pressure range from 1 GPa to 15 GPa, the observed length of the O–H bond was too short (which is typical for the X-ray data) so DFIX setting the O–H distance as 0.82 Å was used. Above 20 GPa we observe that the O–H bond is extremely elongated

https://doi.org/10.1180/mgm.2025.10161 Published online by Cambridge University Press

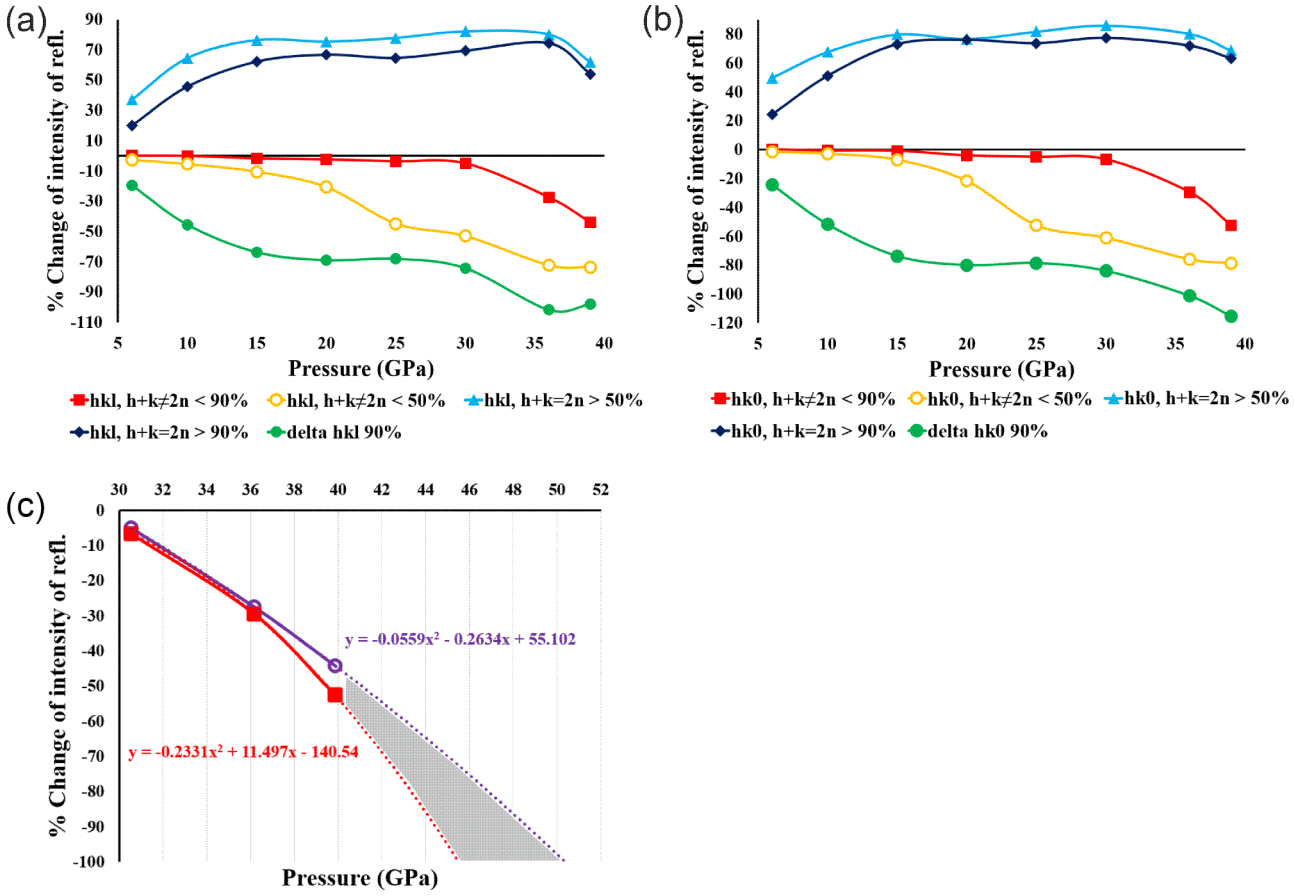


Figure 5. Reflection intensity chart. The light blue line represents the fraction of the reflection, the intensity of which increased by at least 50%. The navy blue line represents the fraction of the reflection, the intensity of which increased by at least 90%. The yellow line represents the fraction of the reflection, the intensity of which decreased by at least 50% and red line, the intensity of which decreased by 90%. The green line represents a comparison of how much the intensity of the group of reflections described by the red line decreases relative to the reflections described by the navy blue line. In (c) is an extrapolation (on the basis of experimental points) showing how quickly the considered group of reflections could disappear completely.

and its value oscillates around 1.2 Å. Simultaneously, the distance between neighbouring O atoms is ~2.4 Å. We believe that it could be explained by the fact that as a result of structure shrinking hydrogen atoms find a position half way to the next neighbouring O atom which is known as symmetrization of hydrogen bonding.

With the increase of pressure, in addition to the above mentioned unit-cell shrinking and deformation of MnO_6 octahedra, another phenomenon becomes more and more visible. We have observed that above 30 GPa specific groups of reflections lose their intensities and disappear. As shown, for example, in Fig. 4, a specific group of reflections that follows the rule $hk0\ h + k = 2n + 1$ is partly absent.

The main question which needs to be answered is why some reflections lose their intensity. We see that there is a certain particular pattern in it. Reflections, which are disappearing, are not random. In fact, decreasing intensities of reflections are associated with certain groups of them. This may indicate that they are affected by the pressure crystal structure when it just starts to change in a certain direction. Can one predict in which direction this change is heading? Analysis of the groups of weakening reflections allows us to assume that the unit cell changes from the primitive (*P*-lattice) to the base-centred (*C*-lattice) one. This also will be accompanied by the appearance of additional symmetry elements. When we assume that all the groups of reflections, which are significantly less intense, will disappear completely, then reflection extinction conditions for the *Cmcm* space group will be fulfilled. We have to underline here that at 39 GPa pressure, the reflections conditions for the *Cmcm* space group are not yet fully met, however we already have reasons to consider if the phase transition

Table 4. Details pertaining to the intensity data collections and structure refinements of groutite in *Pbnm* phase at different pressures (λ = 0.41691 Å)

	p8	p9
P (GPa)	36.15(8)	39.85(8)
	Pbnm	*Pbnm*
Merged runs	9	12
Measured reflections	3129	3647
Unique reflections	341	442
Observed refl. $I > 2\Sigma(I)$	304	313
*R*int	0.045	0.061
Max. 2θ (°)	26.1	26.1
$(\sin\theta/\lambda)_{max}$ (Å^{-1})	1.054	1.055
No. of l.s. parameters	20	23
$R1$, $I > 2\Sigma(I)$	0.033	0.091
*wR*2	0.090	0.238
GooF	1.16	5.54
Residuals (*e*–/Å^3)	0.74, −1.06	1.59, −2.53

https://doi.org/10.1180/mgm.2025.10161 Published online by Cambridge University Press

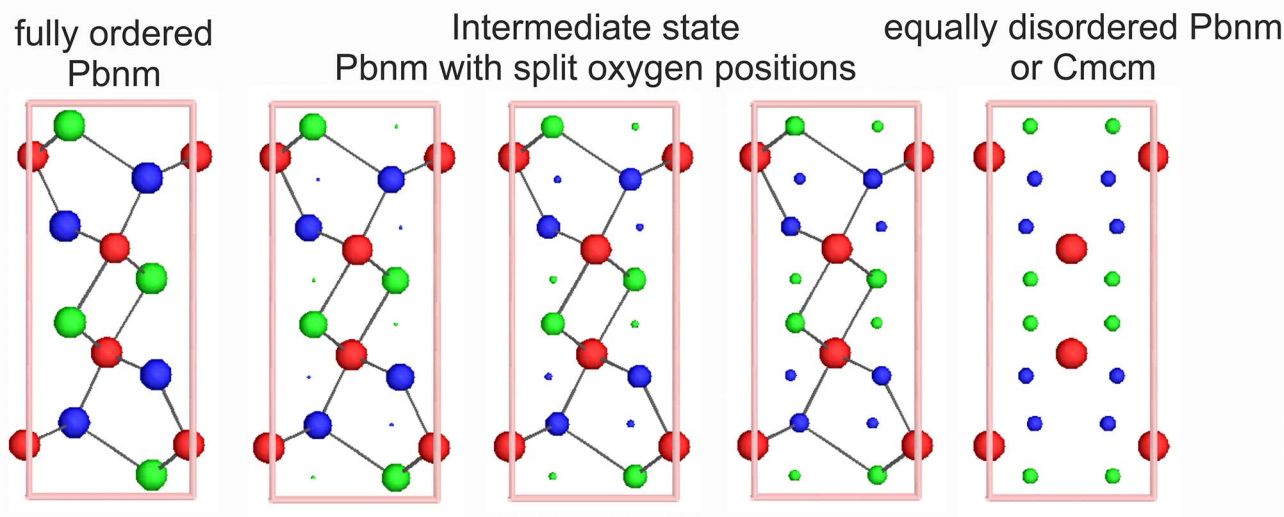


Figure 6. Steps of transformation between *Pbnm* and *Cmcm* space group. Red circles – Mn, green circles – O1, blue circles – O2. View along [001] direction.

from *Pbnm* to *Cmcm* is possible and likely in this structure. We decided to refine the groutite structure before the transformation in *Pbnm* rather than *Pnma*, as this allows for a direct comparison of the unit cells in *Pbnm* and *Cmcm* without requiring any unit cell transformation.

Examples of phase transitions in minerals between the space groups *Pbnm* and *Cmcm* are known in the literature. One of the best studied example is SnSe, which undergoes a high-pressure phase transition from *Pbnm* to *Cmcm* under ca. 2.5 GPa (Ivanova *et al.*, 2018; Aseginolaza *et al.*, 2019). More than 100 scientific papers describing different aspects of phase transition in this layered semiconductor have been published so far, which shows how this structure could be transferred, including in seemingly simple arrangements.

When we examine the Bragg peaks within the investigated pressure range, we observe that their intensities can change significantly. To systematize this issue, we decided to focus primarily on groups of reflections that are crucial for understanding a potential phase transition from *Pbnm* to *Cmcm*. Because the sample is placed in a pressure cell, which limits access to the reciprocal space, not every group of reflections is well represented in the list of all measured reflections. Additionally, the particular orientations of the measured single crystals affects the list of reflections. Therefore, we decided to first consider reflections that either fulfil or do not fulfil the following conditions: *hkl* $h + k = 2n$ and its subgroup *hk0* $h + k = 2n$. The first general condition *hkl;* $h + k = 2n$ is true for the *Cmcm* space group, but does not occur in *Pbnm*. This means that if there is no phase transition, reflections that do not fulfil this condition should still be visible. When these reflections disappear, this may suggest that a phase transition is occurring. This is obviously also true for the subgroup *hk0* $h + k = 2n$, but in this case, we can also quickly verify it by visually inspecting the reconstruction of the reciprocal lattice planes 0*Y*Z *0kl* (see Fig. 4)

To track absent reflections and intensity changes we applied two intensity thresholds: 50% and 90% (for details see Supplementary material) and compared the intensities of reflections at each pressure point to the reference pressure (p1) (see Fig. 5). We observe that at 15 GPa, in both investigated groups of reflections, *hkl* $h + k \neq 2n$ and *hk0* $h + k \neq 2n$, a significant proportion of reflections show intensities that are weakened by at least 50%, and this proportion increases with pressure. To estimate the fraction of absent reflections, we used a threshold of 90%. This means that when the intensity of a particular reflection decreases by at least 90%, we treat it as practically absent. As we can see from Fig. 5, after 30 GPa, the fraction of Bragg peaks weakened by 90% or more increased sharply. We believe that above 30 GPa, the transformation from *Pbnm* to *Cmcm* begins, and the percentage of Bragg peaks *hkl* $h + k \neq 2n$ and *hk0* $h + k \neq 2n$ is a good indicator of this process.

Refinements of the groutite structure for two pressure points: 36.15(8) GPa and 39.85(8) GPa are presented in Table 4. At these pressure points, the percentage of reflections from the considered groups, whose intensities have weakened by 90% or more, varies between 40% and 50%. This is why it is still possible to refine the structures in the 'old' space group *Pbnm*, as ∼50% of reflections that should be forbidden in *Cmcm* are still observed, although significantly weakened. As ∼50% of the reflections forbidden in the *Cmcm* space group have already been significantly weakened or are not observed, we cannot yet refine the structure in the *Cmcm* space group, but we do it instead in a so called intermediate stage, which is the *Pbnm* space group with split oxygen positions (see Table 4).

We used *Isodistort* software (Campbell *et al.*, 2006) to visualize what the reverse phase transition from *Cmcm* space group (as a parent) to *Pbnm* (as a child) might look like. *Isodistort* is a tool for exploring distorted crystal structures in terms of the symmetry modes of the irreducible representations of the parent space-group symmetry. A distorted (child) structure, in our case groutite in the *Pbnm* space group, can be described as a symmetry-lowering deviation from an undistorted reference (parent) structure, in our case groutite in the *Cmcm* space group. The transformation of the groutite crystal structure between *Cmcm* and *Pbnm* is shown in Fig. 6. In our case, at the beginning, we have the ordered structure of groutite in the *Pbnm* space group. This corresponds to our refinement results from pressure points within the range from 1 GPa to 30 GPa.

At 39 GPa pressure, it is possible to solve the structure still in the *Pbnm* space group but already in a slightly different way. Let us call this stage an 'intermediate step'. We have still the *Pbnm* symmetry but already have the split positions of the oxygen atoms as

https://doi.org/10.1180/mgm.2025.10161 Published online by Cambridge University Press

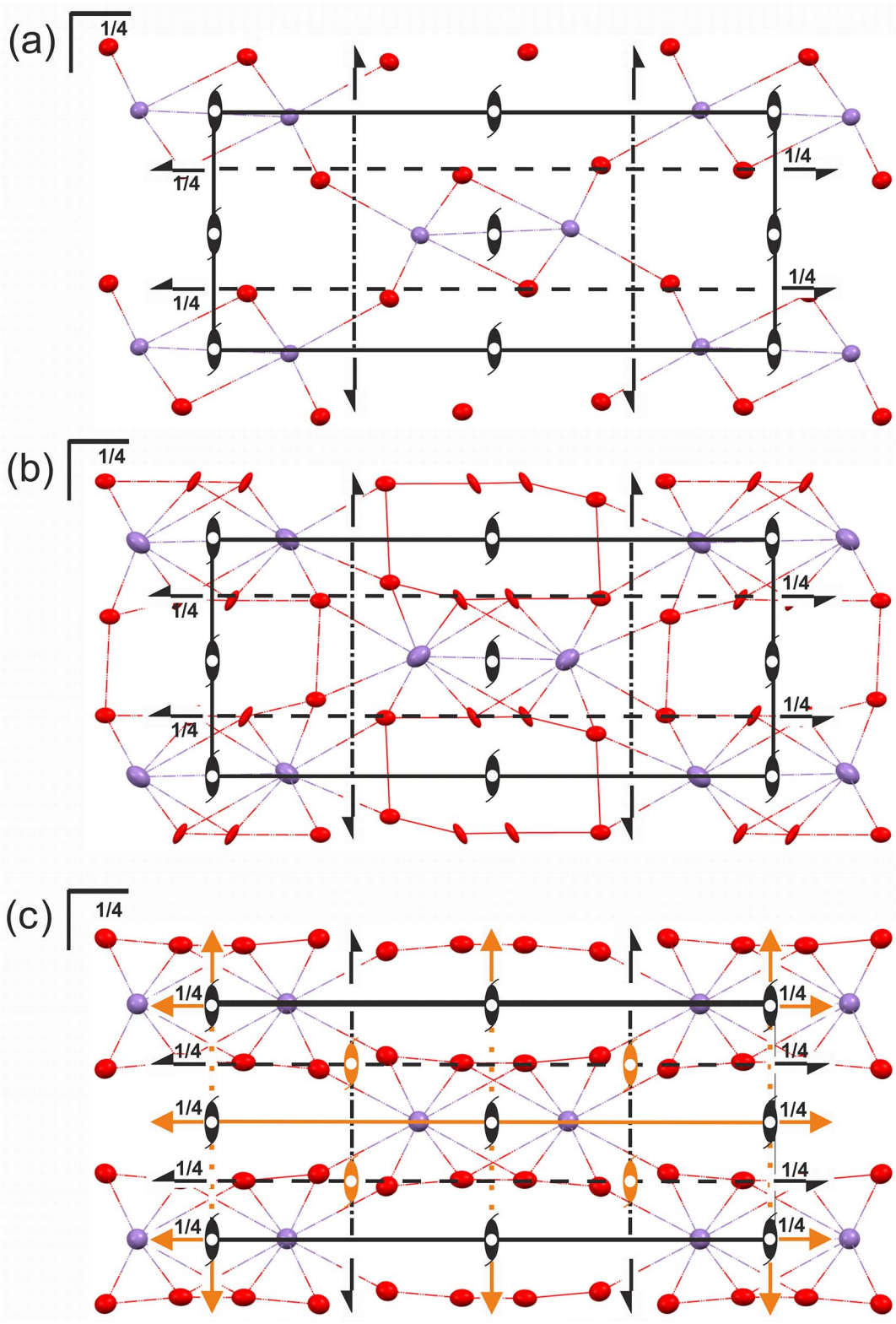


Figure 7. The packing diagram of groutite: (a) at 30 GPa (*Pbnm*) with symmetry elements; (b) 39 GPa (*Pbnm*) with split positions of oxygen atoms; (c) potential equal ratio of the split oxygen positions at some point with higher pressure would allow refinement of the structure in *Cmcm*. View along the [001] direction. The symmetry elements which appear in *Cmcm* but are not observed in *Pbnm* are coloured orange. Hydrogen atoms are omitted for clarity. Ellipsoids of anisotropic displacement parameters at 75% level.

this is the case in the *Cmcm* space group. Positions of the oxygen atoms could be refined as split ones with the ratio 80:20. We can estimate that at some higher pressure values, this ratio will achieve 50:50. This disorder allows us to turn towards a new phase.

https://doi.org/10.1180/mgm.2025.10161 Published online by Cambridge University Press

A potential situation, where oxygen atom positions are split in a 50:50 ratio means complete extinction of previously weakened reflections (reflection conditions for *Cmcm* are fully met) and possibility of refinement in the *Cmcm* space group. As we see from Fig. 5d, where lines showing disappearing groups of reflections are extrapolated to the higher values of pressure, such a situation could probably occur somewhere within the pressure range 45 GPa to 50 GPa. However, it is just a prediction on the basis of very few experimental points. A movie presenting the transformation depicted in Fig. 6 is provided as a separate mp4 file in the Supplementary information.

The high-pressure phase transition of the groutite structure from the *Pbnm* to the intermediate stage (*Pbnm* with split oxygen atoms) and then further to a potential *Cmcm* space group, as postulated by us, requires a more in-depth explanation. First of all, this appears to be more of a continuous process than a sharp event. Initially, it is 80:20 at 39 GPa. However, to meet *Cmcm* requirements it should be finally a 50:50 ratio. In the initial *Pbnm* space group, each oxygen atom is characterized by the *m* site symmetry and a site occupancy factor (sof) of 1 (Wyckoff position 4*c*). In the expected final result of the transformation, the *Cmcm* space group, the sof changes to 0.5, and the Wyckoff position shifts to 8*g*. A slight shift of the manganese atom is also observed, with its site symmetry in *Cmcm* changing from *m* (in *Pbnm*) to *m*2*m*. As a result, additional symmetry elements are allowed to appear in the unit cell (see Fig. 7). Because the oxygen atom position is split, it seems that the atomic position of the hydrogen atom should split as well. However, on the basis of collected data, we were unable to determine and refine stable and reasonable split positions of a possibly disordered hydrogen atom in the intermediate stage (Pbnm with split oxygen atoms, p9).

Conclusions

A smooth, continuous shrinkage in the unit cell volume (∼19.5% from 0.65(6) GPa to 39.85(8) GPa) is a direct result of the pressure increase. This reduction in volume is accompanied by distortion of MnO_6 octahedra. Up to ca 30 GPa we observe just the expected results of the rising pressure. However, above ca 30 GPa, certain Bragg reflections that are allowed in the *Pbnm* phase become progressively absent as pressure increases. It may suggest a forthcoming phase transition.

At 39 GPa, it is still possible to solve the structure in the Pbnm space group but already with split positions of the oxygen atoms. At this stage, the split ratio is still unequal (80:20). The simulations in *Isodistort* shows that when the split ratio achieves 50:50, the lattice will be fully corresponding to the base-centred unit cell. At this pressure point, the phase transition from *Pbnm* to *Cmcm* should be completed with all reflections corresponding to the *Pbnm* symmetry probably absent. The continuous nature of the transition suggests that groutite's crystal structure evolves gradually under pressure, with the transformation from an ordered to a disordered structure.

This study underscores the importance of monitoring reflection intensities and symmetry changes as a function of pressure when studying high-pressure phase transitions. The findings could have broader implications for understanding the behaviour of manganese oxide minerals under extreme conditions, which could inform both mineralogical and industrial applications, such as in the development of new materials under high-pressure environments.

Supplementary material. The supplementary material for this article can be found at https://doi.org/10.1180/mgm.2025.10161.

Acknowledgements. Support for this work provided by the National Science Centre, Poland (OPUS grant No. UMO-2019/33/B/ST10/02671 awarded to KW) is gratefully acknowledged. This work was partly carried out at the Biological and Chemical Research Centre, University of Warsaw, established within a project co-financed by the European Union through the European Regional Development Fund under the Operational Program Innovative Economy, 2007–2013. The research was conducted at the TEAM TECH Core Facility for crystallographic and biophysical research, which supports the development of medicinal products, sponsored by the Foundation for Polish Science (FNP). We also acknowledge SOLEIL for providing synchrotron radiation facilities. The experiment was conducted at beamline CRISTAL, proposal number 20231567.

Competing interests. The authors declare none.

References

Aseginolaza U., Bianco R., Monacelli L., Paulatto L., Calandra M., Mauri F., Bergara A. and Errea I. (2019) Phonon Collapse and Second–Order Phase Transition in Thermoelectric SnSe. *Physical Review Letters*, **122**, 075901.

Campbell B.J., Stokes H.T., Tanner D.E. and Hatch D.M. (2006) *ISODISPLACE*: a web-based tool for exploring structural distortions. *Journal of Applied Crystallography*, **39**, 607–614.

Collin R. and Lipscomb W. (1949) The Crystal Structure of Groutite, Hmno2. *Acta Crystallographica*, **2**, 104–106.

CrysAlis Pro (2014) *CrysAlis Pro*. Agilent Technologies Ltd, Yarnton, Oxfordshire, England.

Dolomanov O.V., Bourhis L.J., Gildea R.J., Howard J. a. K. and Puschmann H. (2009) OLEX2: a complete structure solution, refinement and analysis program. *Journal of Applied Crystallography*, **42**, 339–341.

Evans H. and Block S. (1953) The Crystal Structure of Montroseite, a Vanadium Member of the Diaspore Group. *American Mineralogist*, **38**, 1242–1250.

Evans H. and Mrose M. (1955) A Crystal Chemical Study of Montroseite and Paramontroseite. *American Mineralogist*, **40**, 861–875.

Friedrich A., Wilson D.J., Haussuehl E., Winkler B., Morgenroth W., Refson K. and Milman V. (2007a) High-pressure properties of diaspore, AlO(OH). *Physics and Chemistry of Minerals*, **34**, 145–157.

Friedrich A., Haussuehl E., Boehler R., Morgenroth W., Juarez-Arellano E.A. and Winkler B. (2007b) Single-crystal structure refinement of diaspore at 50 GPa. *American Mineralogist*, **92**, 1640–1644.

Gajda R., Parafiniuk J., Fertey P., Dera P. and Wozniak K. (2024) Electron density changes accompanying high-pressure phase transition in AlOOH. *Mineralogical Magazine*, **88**, 288–301.

Glasser L.S.D. and Ingram L. (1968) Refinement of the crystal structure of groutite MnOOH. *Acta Crystallographica Section B–Structural Crystallography and Crystal Chemistry*, **24**, 1233–1236.

Gonzalez-Platas J., Alvaro M., Nestola F. and Angel R. (2016) EosFit7–GUI: a new graphical user interface for equation of state calculations, analyses and teaching. *Journal of Applied Crystallography*, **49**, 1377–1382.

Gruner J. (1947) Groutite, Hmno2, a New Mineral of the Diaspore–Goethite Group. *American Mineralogist*, **32**, 654–659.

Gualtieri A.F. and Venturelli P. (1999) In situ study of the goethite–hematite phase transformation by real time synchrotron powder diffraction. *American Mineralogist*, **84**, 895–904.

Hellenbrandt M. (2004) The Inorganic Crystal Structure Database (ICSD)—Present and Future. *Crystallography Reviews*, **10**, 17–22.

Hill R. (1979) Crystal-Structure Refinement and Electron-Density Distribution in Diaspore. *Physics and Chemistry of Minerals*, **5**, 179–200.

Ivanova A.G., Troyan I.A., Chareev D.A., Gavriliuk A.G., Starchikov S.S., Baskakov A.O., Frolov K.V., Mezouar M. and Lyubutin I.S. (2018) Structural Phase Transitions and the Equation of State in SnSe at High Pressures up to 2 Mbar. *Jetp Letters*, **108**, 414–418.

Jacobsen S.D., Holl C.M., Adams K.A., Fischer R.A., Martin E.S., Bina C.R., Lin J.-F., Prakapenka V.B., Kubo A. and Dera P. (2008) Compression of single-crystal magnesium oxide to 118 GPa and a ruby pressure gauge for helium pressure media. *American Mineralogist*, **93**, 1823–1828.

Ketkaew R., Tantirungrotechai Y., Harding P., Chastanet G., Guionneau P., Marchivie M. and Harding D.J. (2021) OctaDist: a tool for calculating distortion parameters in spin crossover and coordination complexes. *Dalton Transactions*, **50**, 1086–1096.

Kohler T., Armbruster T. and Libowitzky E. (1997) Hydrogen bonding and Jahn–Teller distortion in groutite, α-MnOOH, and manganite, γ-MnOOH, and their relations to the manganese dioxides ramsdellite and pyrolusite. *Journal of Solid State Chemistry*, **133**, 486–500.

Komatsu K., Kuribayashi T., Sano A., Ohtani E. and Kudoh Y. (2006) Redetermination of the high-pressure modification of AlOOH from single-crystal synchrotron data. *Acta Crystallographica Section E–Crystallographic Communications*, **62**, I216–I218.

Kvasnytsya V.M. and Naumenko E.V. (2017) Crystal morphology of groutite (α-MnOOH) from the Zavallya graphite deposit (The Ukrainian shield). *Mineralogical Journal–Ukraine*, **39**, 11–18.

Liu K., Dai L., Li H., Hu H., Zhuang Y., Yang L., Pu C. and Hong M. (2019) Pressure-induced phase transitions for goethite investigated by Raman spectroscopy and electrical conductivity. *High Pressure Research*, **39**, 106–116.

Lufaso M.W. and Woodward P.M. (2004) Jahn–Teller distortions, cation ordering and octahedral tilting in perovskites. *Acta Crystallographica Section B: Structural Science*, **60**, 10–20.

Petricek V., Palatinus L., Plasil J. and Dusek M. (2023) JANA2020-a new version of the crystallographic computing system JANA. *Zeitschrift Fur Kristallographie–Crystalline Materials*, **238**, 271–282.

Post J.E., Heaney P.J., Ilton E.S. and Elzinga E.J. (2023) The crystal structure of feitknechtite (β-MnOOH) and a new MnOOH polymorph. *American Mineralogist*, **108**, 2131–2141.

Scheinost A.C., Stanjek H., Schulze D.G., Gasser U. and Sparks D.L. (2001) Structural environment and oxidation state of Mn in goethite–groutite solid-solutions. *American Mineralogist*, **86**, 139–146.

Schlüter J., Klaska K.H., Adiwidjaja G. and Gebhard G. (2003) Tsumgallite, GaO(OH), a new mineral from the Tsumeb mine, Tsumeb, Namibia. *Neues Jahrbuch Fur Mineralogie–Monatshefte*, 521–527.

Sheldrick G.M. (2008) A short history of SHELX. *Acta Crystallographica Section A*, **64**, 112–122.

Sheldrick G.M. (2015) Crystal structure refinement with SHELXL. *Acta Crystallographica Section C – Structural Chemistry*, **71**, 3–8.

Warr L.N. (2021) IMA–CNMNC approved mineral symbols. *Mineralogical Magazine*, **85**, 291–320.

Wiethoff F., Grevel K.-D., Marler B., Herrmann J., Majzlan J., Kirste J. and Lathe C. (2017) *P–V–T* behavior of FeO(OH) and MnO(OH). *Physics and Chemistry of Minerals*, **44**, 567–576.

Zhao D., Xu J., Zhang B., Kuang Y., Fan D., Zhou W., Li X. and Xie H. (2017) Compressibility of natural manganite at high pressure: Influence of Jahn–Teller effect and hydrogen bond. *High Temperatures–High Pressures*, **46**, 61–79.

https://doi.org/10.1180/mgm.2025.10161 Published online by Cambridge University Press